CRACK GROWTH RESISTANCE SIMULATION IN THE MODIFIED BOUNDARY LAYER MODEL WITH A DAMAGE MODEL

A.H.M. Krom*, R.W.J. Koers†, and A. Bakker*

Detailed finite element calculations based on the modified Gurson model were carried out in the boundary layer model to determine parametric crack growth resistance curves (J_R-curves). These curves coincide when the J-integral is scaled by element size and reference stress σ_0 and the crack growth by element size. So crack growth resistance curves are self-similar. This is not the case in the modified boundary layer model. The effect of a negative biaxiality is to give higher initiation J-values and higher resistance to crack growth. The effect of a positive biaxiality is opposite but less pronounced. It is concluded that, in combination with the Gurson model, the modified boundary layer model is suitable for investigating geometry effects on crack growth initiation and resistance.

INTRODUCTION

The damage process in ductile metals which results in cracking involves the nucleation, growth, and coalescence of voids. For ductile crack growth simulations a constitutive model is needed that can describe this damage process. The modified Gurson model, in which the void volume fraction is the most important parameter, can describe this process. For example, Sun et al. (1) have used the modified Gurson model to predict load-displacement and crack growth resistance curves. However, they found that the calculations were dependent on a length parameter which they related to a micro-structural length.

In the modified Gurson model, nucleation and growth of voids are taken into account along with the effect of the void volume fraction on the yield surface. The model has

* Materials Science Laboratory
Delft University of Technology
P.O. Box 5025
2600 GA Delft, The Netherlands

† Shell Research Arnhem
P.O. Box 40
6800 AA Arnhem, The Netherlands

many parameters which must be determined by experimental and numerical methods. Whereas the model takes into account the influence of voids, it does not actually model the voids. When such a damage model is used in the finite element method, we need an appropriate definition of crack growth. Somehow this will be related to the element size. In real metals, crack growth corresponds to a micro-structural length. In many studies the effect of element size is not reported or not quite clear. We carried out detailed finite element calculations in a geometry independent model (the boundary layer model) in order to investigate the influence of element size. In the boundary layer model a cracked body with a plastic zone around the crack tip is replaced by a semicircular region with boundary conditions corresponding to the applied values of stress intensity. By modifying the boundary layer model with the biaxiality parameter (T-stress), the influence of geometry can be investigated.

In this paper we have determined crack growth resistance curves which give the J-integral as a function of crack growth Δa for different element sizes, and biaxialities.

THEORY

An elastic-plastic material model that accounts for the nucleation and growth of microscopic voids in a ductile metal was developed by Gurson (2) on the basis of the work of Berg (3). The model uses a yield condition for a void-containing material which is derived on the basis of approximate, rigid-perfectly plastic calculations for special void geometries. This yield condition is of the form $\Phi(\sigma, \sigma_M, f)=0$, where σ is the average macroscopic Cauchy stress, σ_M is an equivalent tensile flow stress representing the actual microscopic stress state in the matrix, and f is the current void volume fraction. In this paper we employ the modified Gurson yield function,

$$\Phi = \frac{\sigma_e^2}{\sigma_M^2} + 2qf^* \cosh\left(\frac{3\sigma_m}{2\sigma_M}\right) - \left\{1 + \left(qf^*\right)^2\right\} = 0 \quad \ldots\ldots (1)$$

where $\sigma_e^2 = 3/2 s_{ij}s_{ij}$ is the macroscopic equivalent stress, and $\sigma_m = 1/3\sigma_{kk}$ the mean stress, with $s_{ij} = \sigma_{ij} - 1/3\sigma_{kk}\delta_{ij}$ the stress deviator, and with δ_{ij} the Kronecker delta. The average actual microscopic stress state in the matrix material is represented by an equivalent flow stress σ_M. For $f^*=f$ and $q=1$, Eqn. (1) reduces to the original Gurson yield function. The additional parameter q was introduced by Tvergaard (4) to bring predictions at low volume fractions in a closer agreement with cell model calculations. As discussed by Tvergaard and Needleman (5), the complete loss of material stress-carrying capacity at ductile fracture due to the coalescence of voids, is not predicted at a realistic level of the void volume fractions by the Gurson model.

To overcome this difficulty, they introduced the function $f^*(f)$ which takes into account the coalescence of voids:

$$f^*(f) = \begin{cases} f & , \text{for } f \le f_c \\ f_c + \dfrac{f_u^* - f_c}{f_F - f_c}(f - f_c) & , \text{for } f > f_c \end{cases} \quad \ldots\ldots (2)$$

so below f_c the void volume fraction is unchanged and above f_c the function is as if the void volume fraction is higher than in reality. The change of void volume fraction during an increment of deformation is given by:

$$\dot{f} = \dot{f}_{growth} + \dot{f}_{nucleation} \quad \ldots\ldots (3)$$

where $\dot{f}_{growth}$ is the change in void volume fraction due to growth of existing voids, and $\dot{f}_{nucleation}$ the change due to the nucleation of voids. Because of the plastic incompressibility of the matrix the change in volume is to account for the change in void volume. Therefore, $\dot{f}_{growth}$ is related to the plastic volume strain rate as follows:

$$\dot{f}_{growth} = (1 - f)\dot{\varepsilon}^p_{kk} \quad \ldots\ldots (4)$$

The $\dot{f}_{nucleation}$ can be stress controlled, strain controlled, or both. As proposed by Chu and Needleman (6) the nucleation rate can be described by a normal distribution. We have chosen for a nucleation rate that is controlled by stress, as follows:

$$\dot{f}_{nucleation} = \left(\dot{\sigma}_M + \frac{\dot{\sigma}_{kk}}{3}\right)\frac{f_{N\sigma}}{s_\sigma\sqrt{2\pi}}\exp\left[-\frac{1}{2}\left\{\frac{\left(\sigma_M + \dfrac{\sigma_{kk}}{3}\right) - \sigma_N}{s_\sigma}\right\}^2\right] \quad \ldots\ldots (5)$$

where $f_{N\sigma}$ is the volume fraction of the void nucleating particles, s_σ the standard deviation of the stress over which most of the voids nucleate, $\sigma_M + 1/3\sigma_{kk}$ a measure of the maximum stress at the interface.

The modified boundary layer model is used to investigate geometry and loading effects on near crack tip fields without the need to model the complete geometry. The origin of the modified boundary layer model is in the small-scale yielding situation. Infinitely far from the tip of a semi-infinite crack, stresses and strains are controlled by the elastic singularity: the mode I stress intensity factor K_I. This, however, is only true when the plastic zone is infinitely small. In the boundary layer model are no

natural length parameters, the model is geometry independent. Larsson and Carlsson (7) modified the boundary layer model with the T-stress to account for geometry and loading effects. As a consequence the formulation becomes geometry dependent. The modified boundary layer model in terms of stresses is given by:

$$\sigma_{ij} = \frac{K_I}{\sqrt{2\pi r}} f_{ij}(\theta) + T\delta_{1i}\delta_{1j} \quad \ldots\ldots (6)$$

where r and θ are cylindrical co-ordinates with the crack tip as their origin. The T-stress is related to the stress intensity factor by the biaxiality parameter B:

$$B = \frac{T\sqrt{\pi a}}{K_I} \quad \ldots\ldots (7)$$

where a is the crack length. The biaxiality parameter depends on crack length, geometry, and loading. Generally speaking, B is positive for bend specimens and negative for tensile specimens.

METHOD

Calculations were done using the finite element program MARC, version K5.2, on a DEC Alpha workstation. In this program the modified Gurson model is implemented. A large displacement, finite deformation and updated Lagrange method were used. The finite elements used were 4-node plane strain isoparametric quadrilaterals with a constant dilatation correction in order to avoid artificial constraints. The mesh is of the 'spider web' type, see Fig. 1. To model the fields near the crack tip the elements near the crack are small compared to the elements near the boundary.

To investigate the effect of element size we used three meshes in which only the size of the near tip elements is different. With R the radius of the web and L the size of elements near the crack tip, the sizes of the elements L/R=0.2 10^{-3}, 0.1 10^{-3}, and 0.05 10^{-3}, respectively. The meshes consist of 778, 950, and 1147 elements, respectively. A detail near the crack tip of the finest mesh is shown in Fig. 2. Plane strain displacements on the boundary are prescribed according to Bilby et al (8).

The condition $f^*=0.9/q$ (or equivalently $f=0.9f_F$) was used instead of $f=1/q$ in order to avoid numerical instabilities when f^* approaches 1/q. As the void volume fraction reaches this value in one of the four integrations points, the element stiffness is reduced to zero (deactivated). Then the element is considered to be cracked and the crack has grown by an amount of L (undeformed mesh). So contraction of the element is not taken into account. When the first element ahead of the crack tip is

deactivated, the crack tip node is not released. Therefore, the element behind the crack tip is also deactivated. Although the criterion for crack growth is determined from one of the integration points, the average void volume fraction varied less from the 90% value at fracture except for the first two cracked elements.
The J-integral is determined by the virtual crack extension method according to Bakker (9). The J-integral is determined in the second path of elements from the outer radius.
The material behaviour is given by a uniaxial stress-strain curve:

$$\varepsilon = \begin{cases} \dfrac{\sigma}{E} & , \text{ for } \varepsilon \le \dfrac{\sigma_o}{E} \\ \dfrac{\sigma_o}{E}\left(\dfrac{\sigma}{\sigma_o}\right)^n & , \text{ for } \varepsilon > \dfrac{\sigma_o}{E} \end{cases} \qquad (8)$$

where ε is the logarithmic strain, σ the true stress, E the Young's modulus, σ_o a reference stress (the uniaxial yield stress), and n the strain-hardening exponent. The material parameters are $E/\sigma_o=500$, Poisson's ratio, $\nu=0.3$, and $n=5$. Partly following the cell model calculations of Koplik and Needleman (10) we used the following parameters of the Gurson model: $q=1.25$, $f_c=0.03$, $f_F=0.15$, $f_{N\sigma}=0.001$, $\sigma_N=3\sigma_o$, and $s_\sigma=0.5\sigma_o$.

RESULTS

In Fig. 3 the stress normal to the ligament, σ_{22}, is shown as a function of the distance to the (moving) crack tip at different loads. At low loads the crack remains sharp but due to plasticity and void growth the crack tip blunts. As a consequence, the high constraint at the crack tip is lost, and the maximum normal stress is limited and the position of this maximum shifts from the crack tip. After significant crack growth, the position of the maximum does not change. The maximum normal stress is approximately the same as found by McMeeking (11) who carried out calculations in the boundary layer model for a non growing crack. McMeeking found a upturn in the stress distribution near the crack tip due to strain hardening. This, of course, did not occur in our calculations due to the softening caused by damage.

Fig. 4 shows the void volume fraction in the ligament. Clearly, the void volume distribution does not change after crack growth, and that the void fraction development is restricted to a few elements. Moreover, we observed that the void growth is confined to the elements along the ligament. Therefore, we could limit the modified Gurson model to a region near the ligament.

In Fig. 5 the crack growth resistance curves are shown as a function of element size for B=0. Because the element size is the only constant length parameter during the crack growth, the element size is chosen for normalising. In order to have normalised values, the J-integral is normalised by the reference stress σ_0 and the element size L, and the crack growth Δa is normalised by the element size L. As a consequence, the crack growth resistance curves coincide. In fact, this means that the calculations are converged solutions. Furthermore, the J-integral at initiation scales directly with the element size. Another point is that the resistance curves are almost straight except in the beginning. So the slope of the resistance curves depends only slightly on the element sizes used in these calculations. McMeeking (11) found that stress distributions in the boundary layer model coincide when scaled by the J-integral. This means that the stresses are controlled by one parameter: the J-integral. For this effect, McMeeking introduced the term self-similarity. Here, the resistance curves are controlled by the element size. Therefore, we may say that the crack growth resistance curves in the boundary layer model are self-similar.

Fig. 6 shows the crack growth resistance curves for different element sizes and biaxiality. In the modified boundary layer model the crack growth resistance curves depend on biaxiality and element size, and therefore do not coincide. Smaller elements give lower J-integrals at initiation. Thus, the T-stress (Eqn. (7)) is also low and the effect less pronounced than with larger element sizes. So larger elements have greater effects on the resistance curves. The effect of B=-1 is to give a higher J-integral at initiation and a higher slope of the resistance curve. For B=+1 the resistance curve almost coincides with the curve for B=0 (see Fig. 5). So the effect of B=+1 is much less pronounced. This effect is similar to the one Bilby et al (8), found for the stress distribution for a non growing crack in the modified boundary layer model.

CONCLUSIONS

Using the Gurson model in the finite element method it follows that crack initiation and growth depend on element size L. It is observed that the J-integral at initiation (cracking of the first element) scales directly with the element size in the boundary layer model. When the J-integral is scaled by element size and reference stress σ_0 and the crack growth by element size, the crack growth resistance curves coincide. So crack growth resistance curves are self-similar.

The effect of a negative biaxiality (simulating specimens loaded in tension) is to give a higher initiation J-integral and higher resistance to crack growth, which corresponds with experimental observations. The effect of a positive biaxiality

(simulating, for example, a compact tension specimen) is opposite but less pronounced. This, too, corresponds with experimental observations.
By modifying the boundary layer model with the biaxiality parameter, the self-similarity of the crack growth resistance curves is lost.

It is concluded that the modified boundary layer model, in combination with the modified Gurson model, is suitable for investigating geometry effects on crack growth initiation and resistance. Further studies should be aimed at determining the various parameters in the modified Gurson model.

REFERENCES

(1) D.-Z. Sun, Voss, B. and Schmitt, W., Defect Assessment in Components - Fundamentals and Applications, eds. J.G. Blauel and K.-H. Schwalbe, Mechanical Engineering Publ. Ltd., London, 1991, pp. 447-458.
(2) Gurson, A.L., J. Eng. Mat. Tech., vol. 99, 1977, pp. 2-15.
(3) Berg, C.A., Inelastic Behaviour of Solids, eds. M. F. Kanninen et al., McGraw-Hill, New York, 1970, pp. 641-672.
(4) Tvergaard, V., Int. J. Frac., vol 17, 1981, pp. 389-407.
(5) Needleman, A. and Tvergaard, V., J. Mech. Phys. Solids, vol 32, 1984, pp. 461-490.
(6) Larsson, S.G. and Carlsson, A.J., J. Mech. Phys. of Solids, vol 21, 1973, pp. 263-277.
(7) Chu, C.-C. and Needleman, A., Eng. Mat. Tech., vol 102, 1980, pp. 249-256.
(8) Bilby, B.A., Cardew, G.E., Goldthorpe, M.R. and Howard, I.C., Size Effects in Fracture, Mechanical Engineering, London, 1986, 37-46.
(9) Bakker, A., Int. J. Pres. Vess. Piping, vol 14, 1983, pp. 153-179.
(10) Koplik, J. and Needleman, A., J. Mech. Phys. Solids., vol 24, 1988, pp. 835-853.
(11) McMeeking, R.M., J. Mech. Phys. Solids., vol 25, 1977, pp. 357-381.

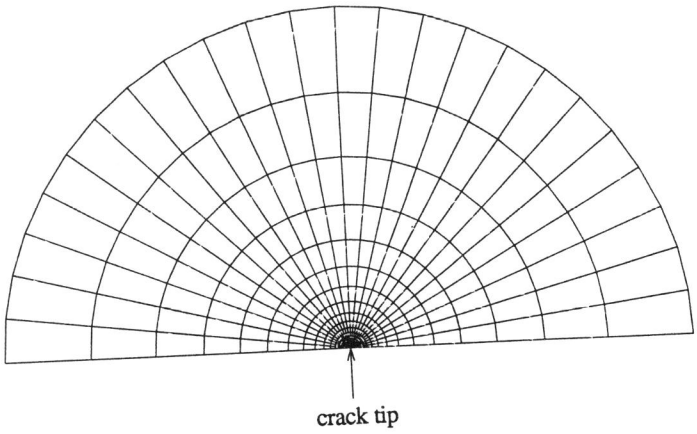

Figure 1 The finite element mesh used for ductile crack growth calculations

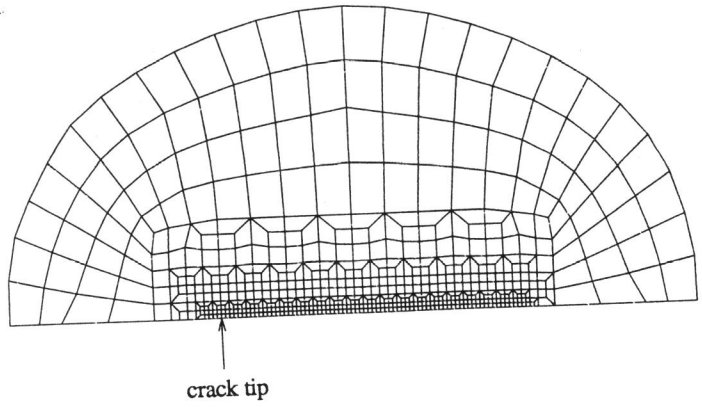

Figure 2 Detail near the crack tip of the finest mesh ($L/R=0.05\ 10^{-3}$)

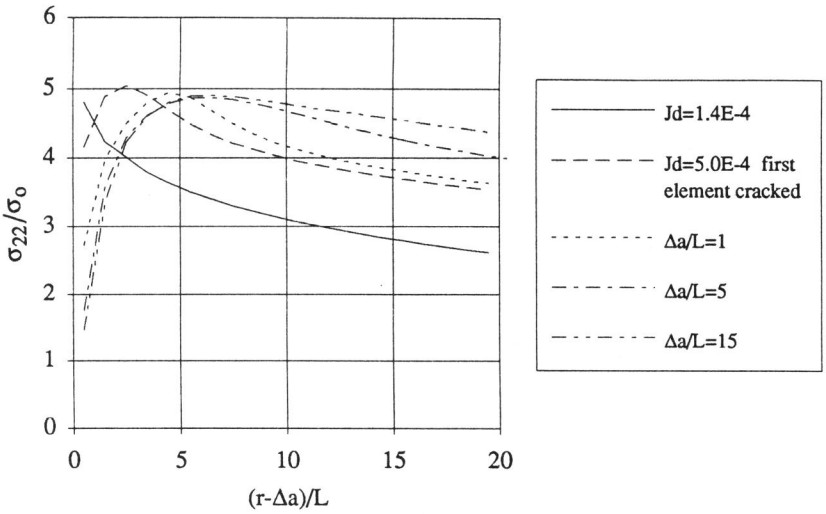

Figure 3 Stress σ_{22} in the ligament ($Jd = J / (\sigma_o a)$, B=0, L/R=0.01 10^{-3})

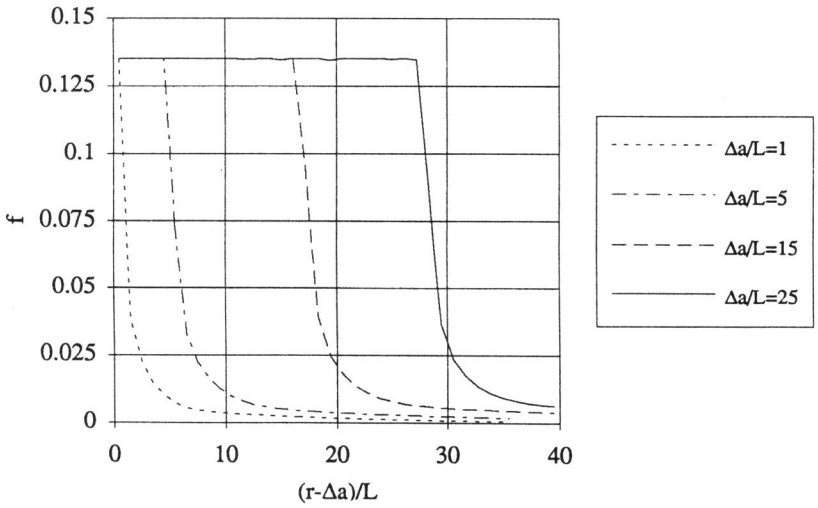

Figure 4 Void volume fraction in the ligament (B=0, L/R=0.01 10^{-3})

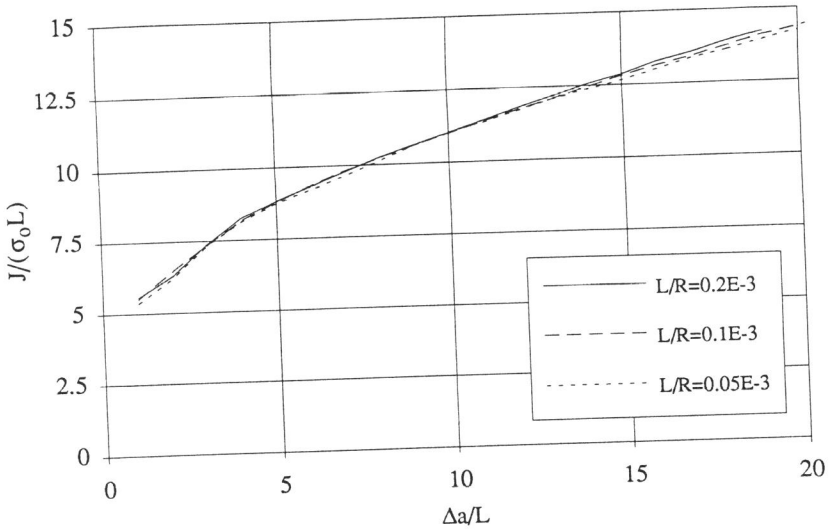

Figure 5 Normalised crack growth resistance curves for three element sizes (B=0, L=element size, R= outer radius of the boundary layer model)

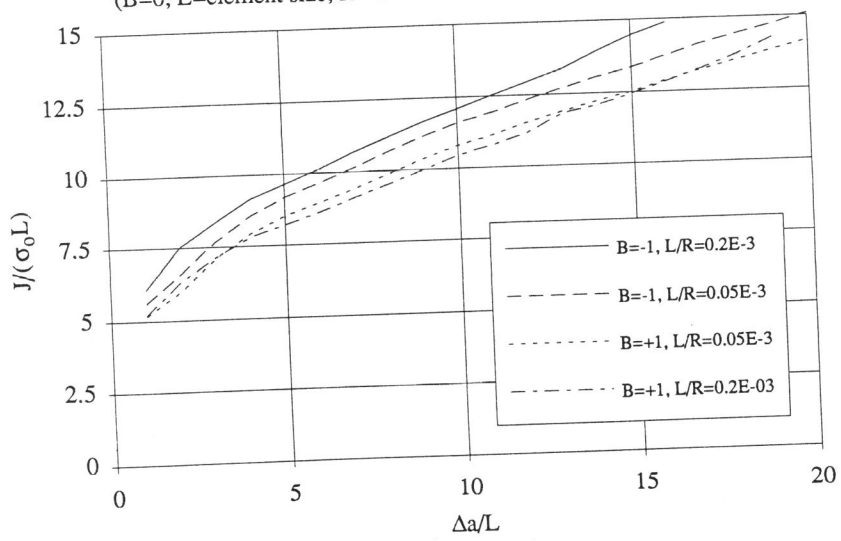

Figure 6 Normalised crack growth resistance curves for element sizes L=0.05, and 0.2, and for biaxiality B= -1, and +1